Numerical study of the spreading and solidification of a molten particle impacting onto a rigid substrate under plasma spraying conditions

Soufiane Oukach, Hassan Hamdi, Mohammed El Ganaoui, Bernard Pateyron

NUMERICAL STUDY OF THE SPREADING AND SOLIDIFICATION OF A MOLTEN PARTICLE IMPACTING ONTO A RIGID SUBSTRATE UNDER PLASMA SPRAYING CONDITIONS

by

Soufiane OUKACH [a,b,c*], Hassan HAMDI [b], Mohammed EL GANAOUI [c], and Bernard PATEYRON [a]

[a] Science of Ceramic Processes and Surface Treatment Laboratory, (SPCTS-UMR 6638 CNRS), European Centre of Ceramics, Limoges, France
[b] Fluid Mechanics and Energetic Laboratory (LMFE -URAC 27 CNRST), Faculty of Sciences Semlalia, Cadi Ayyad University, Marrakech, Morocco
[c] University Institute of Technology of Longwy/LERMAB, University of Lorraine, Cosnes-et-Romain, France

Original scientific paper
DOI: 10.2298/TSCI120730097O

This paper deals with simulation of the spreading and solidification of a fully molten particle impacting onto a preheated substrate under traditional plasma spraying conditions. The multiphase problem governing equations of mass, momentum and energy conservation taking into account heat transfer by conduction, convection, and phase change are solved by using a finite element approach. The interface between molten particle and surrounding air, is tracked using the Level Set method. The effect of the Reynolds number on the droplet spreading and solidification, using a wide range of impact velocities (40-250 m/s), is reported. A new correlation that predicts the final spread factor of splat as a function of Reynolds number is obtained. Thermal contact resistance, viscous dissipation, wettability and surface tension forces effects are taken into account.

Key words: *simulation, level set, droplet impact, multiphase flow, solidification*

Introduction

The plasma spray technology is extensively used in a wide variety of applications (aerospace, automotive, nuclear, *etc*.) to provide functional surfaces. This technique consists of injecting the powdered material (~10-100 μm) into a plasma jet where particles are heated, melted and propelled at high speed toward the surface to be coated on which they flatten, quench rapidly and solidify. Coating is built up when millions of individual splats are cumulatively deposited on the top of each other giving a multilayered structure [1]. During the last three decades, much attention has been given to understanding the nature and microstructure of the resulting coatings. Many researchers have shown that the thermo-mechanical properties of plasma-sprayed coatings are strongly related to the physical contact between the layered splats and that the first layer in contact with the substrate governs the adhesion of the coating to the

* Corresponding author; e-mail: soufiane.oukach@univ-lorraine.fr

substrate [1]. Therefore, a better understanding of the spreading, cooling, and solidification process of an individual droplet impinging onto a substrate is required in order to improve control and quality of coating in deposition process. Furthermore, in plasma spray process, as the spreading and solidification of an individual droplet are complete before the next droplet arrives on the substrate, the solidification of an individual droplet is considered not been affected by other droplets.

The spread factor, ξ, which is defined as the ratio of the wetted surface diameter to the droplet initial diameter, is an important parameter in the process of droplet spreading, knowing that the quality of contact between layers is strongly related to the extent of droplet spreading [2]. This parameter is generally expressed as function of Reynolds number through relationships in the form $x = C\mathrm{Re}^{a}$ [1]. The relationship may also contain the Weber number, but in plasma spray process, the effect of the Weber number may be considered trivial due to the effect of inertia forces which is more important than that of the surface tension [3].

Several works: experimental [4, 5], computational [6-9], and also analytical [10-13] have been performed to understand the process of droplet impact, spreading, and solidification, and also to predict the maximum spread factor as a function of the impact conditions.

One of the earliest models dealing with the maximum spread factor is the Jones model [10]. Based on mass and energy conservation and neglecting the surface tension and solidification effects, he found a correlation expressed as $\xi = 1.16\mathrm{Re}^{1/8}$. The model developed by Madejski [13] is considered in the literature as one of the pioneering works. This model is based on a cylindrical deformation of the droplet taking into account viscous energy dissipation and surface tension effects. It assumes that solidification, which has an important effect on the spreading phenomena, starts at the end of spreading. The outcome of the model is a correlation written as $\xi = M\mathrm{Re}^{1/5}$, where M is a constant equal to 1.2941. The model developed by Yoshida [12] gives also an expression of the spread factor similar in form to that of Madejski's flow model with M equal to 0.83, however the results obtained are 35% underestimated compared to the ones obtained assuming Madejski model. Pasandideh-Fard *et al*. [11] developed an analytical model neglecting the surface tension effects .They then arrived at a simple expression for the maximal spread factor $\xi = 0.5\mathrm{Re}^{0.25}$. The exponent 0.25 is not far from the quoted exponent 0.2 found by the authors of [12,13]. Numerical simulations carried out by several authors have also arrived to similar expressions of the spread factor with different M values, *e. g*. $M = 1.18$ [14], 1.04 [15], 1.0 [16], 0.925 [17], and 0.82 [18].

The literature is, however, poor concerning studies using micrometric droplets with high impact velocities, such as in the case of plasma spray process. Therefore, there is a need in developing useful models for simulations of droplet impact, spreading, and solidification under plasma spray conditions.

The aim of this study is to simulate the fluid flow, heat transfer, and solidification phenomena occurring during the normal impact of a molten alumina particle droplet onto a preheated stainless steel substrate using a finite element method. Numerical simulations are carried out in order to investigate the effect of the Reynolds number on the droplet spreading and solidification. Results are then used to establish a correlation that predicts the spread factor as a function of the Reynolds number under plasma spray conditions.

Numerical model and governing equations

The process of impact, spreading and solidification of a molten droplet impinging onto a solid surface involves fluid flow, heat transfer, and phase change. The model has also to deal with the interface between the droplet and the surrounding gas and between liquid and solid

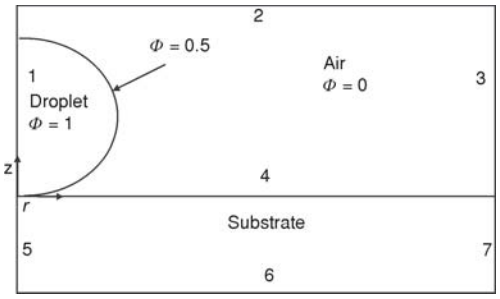

Figure 1. Initial configuration and computational domain. Numeric labels: 1 to 7 refer to boundaries for which conditions are set on tab. 1

Table 1. Boundary conditions

Boundary	Navier-Stokes equations	Heat transfer equation
1	Axial symmetry	Axial symmetry
2, 3	No slip condition	Insulation
4	Wetted wall	Insulation
5	Not active	Axial symmetry
6, 7	Not active	Insulation

phases. The overall impact problem is schematically shown in fig. 1; the boundary conditions are listed in tab. 1.

The fluid flow during the droplet spreading onto the substrate is modeled by using the full Navier-Stokes equations for incompressible flows:

$$\rho\frac{\partial u}{\partial t}+\rho(u\nabla)u=-\nabla p+\nabla\mu[\nabla u+(\nabla u)^T]+\rho g+F_{TS}+F \tag{1}$$

$$\nabla u=0 \tag{2}$$

where u is the velocity, p – the pressure, ρ – the density, μ – the kinematic viscosity, g – the gravitational acceleration, Φ – the term source corresponding to the occurrence of the droplet solidification, and F_{TS} represents the capillary forces given by:

$$F_{TS}=\sigma k\delta n \tag{3}$$

where σ, δ, and k are, respectively, the surface tension coefficient, the Dirac function, and the average local slope of the curve at the liquid-gas interface. n is the normal at the liquid-gas interface.

The Level Set method [19] which is a robust and accurate method, is used to track the evolution of the liquid-gas interface. It is characterized by a stable behavior and good conservation properties. In this method, the interface is represented by a certain level set or iso-contour of a scalar function ϕ. This function ϕ is a smoothed step function that equals (0) in a domain and (1) in its complementary part. Across the interface, there is a smooth transition from (0) to (1) and the interface is represented by the 0,5 iso-contour (fig.1). The function ϕ is advected by the fluid flow according to:

$$\frac{\partial\phi}{\partial t}+u\nabla\phi=\gamma\nabla\left[\varepsilon\nabla\phi-\phi(1-\phi)\frac{\nabla\phi}{|\nabla\phi|}\right] \tag{4}$$

The terms on the left-hand side give the correct motion of the interface, while those on the right-hand side are necessary for numerical stability. The parameters ε and γ determine the thickness of the region and the amount of re-initialization or stabilization of the level set function, respectively, [19].

Both fluids are assumed incompressible and Newtonian, and the surrounding gas (air) has no effect on the deposition process. Any property α of the two fluids at the interface such as density, viscosity or thermal conductivity is expressed as:

$$\alpha=\alpha_{gas}+\phi(\alpha_{liauide}-\alpha_{gas}) \tag{5}$$

The heat exchanges between the droplet, air, and substrate are taken into account by the model using the energy equation:

$$\rho C_p \frac{\partial T}{\partial t} + \nabla(-\lambda \nabla T) = -\rho C_p u \nabla T \tag{6}$$

where T, ρ, and C_p denote, respectively, temperature, density, and specific heat. The term on the right-hand side is introduced to include the convective heat effects. The energy equation is solved in all domains shown in fig. 1.

The thermal contact resistance (*TCR*) is modeled by defining a thin layer of arbitrary thickness l_0 which attaches the two domains (splat and substrate). The effective thermal conductivity k_1 of the splat is related to the *TCR* by eq. (7):

$$k_l = \frac{l_0}{TCR} \tag{7}$$

To analyze the solidification problem, the latent heat related to the solidification must be taken into account. Therefore, in the splat domain, the specific heat C_p in the energy eq. (6) is replaced by:

$$C_p = C_{p_{\text{solide}}} + \frac{H}{T_m} + H\delta \tag{8}$$

where H is the latent heat of transition, T_m the melting temperature, and δ is a Gaussian curve given by:

$$\delta = \frac{\exp\left[-\dfrac{(T - T_m)^2}{(\Delta T)^2}\right]}{\Delta T\sqrt{\pi}} \tag{9}$$

Here ΔT is the temperature interval of phase change.

The source term in eq. (1) is defined in eq. (10) and serves to slow down the velocity of the fluid at the phase-change interface and eventually arrests its motion as the droplet solidifies [20]:

$$F = \frac{(1-\beta)^2}{\beta^3 + \eta} Cu \tag{10}$$

Here C is the mushy zone constant (should have high value to produce a proper damping), η – arbitrary constant (should have small value to prevent division by zero), u – the spreading velocity of the splat, and β – the volume fraction of the liquid phase, given by:

$$\beta = \begin{cases} 0 & T < T_m - \Delta T \\ \dfrac{T - T_m + \Delta T}{2\Delta T} & T_m - \Delta T \le T \le T_m + \Delta T \\ 1 & T > T_m + \Delta T \end{cases} \tag{11}$$

The numerical model is solved using an Eulerian approach in a fixed grid and a Finite Element implemented in COMSOL software. Its validation was presented in [21, 22].

Results and discussion

Figure 2 shows a 2-D axisymmetric representation of deformation and solidification sequence of a single droplet impinging onto a stainless steel substrate with an impact velocity of 40 m/s. The *TCR* and equilibrium contact angle were held constant and set, respectively, to 10^{-7} m^{2}K/W and 70° [23]. Initial conditions and thermo-physical properties of different materi-

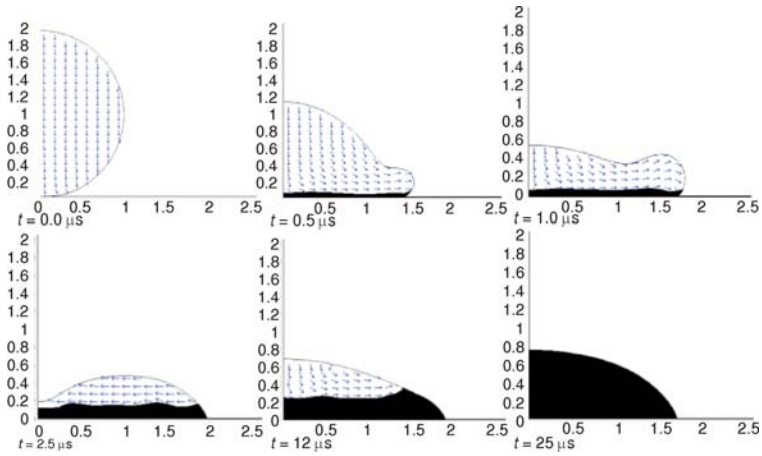

Figure 2. Deformation and solidification sequence of a single droplet impinging onto a stainless steel substrate with an impact velocity of 40 ms^{-1}.The solidified part in the droplet is shown in black and the arrows indicate the sense of fluid motion

als used in this study are listed in tab. 2. The droplet begins to deform once it hits the substrate, its shape starts to change and the liquid begins to expand outwards in the radial direction. Solidification occurs immediately after deformation in the lowest layer of the droplet in contact with the substrate, a plateau forms leading to deceleration of the liquid motion. The droplet reaches its static state after a finite spreading time in the order of a microsecond.

Table 2. Initial conditions and thermo-physical properties of materials used in this study

	Alumina	Air	Stainless steel	Units
Density, ρ	2900	1.3	7850	kgm^{-3}
Viscosity, μ	$12 \cdot 10^{-3}$	$1.7 \cdot 10^{-5}$	–	Pa·s
Surface tension, σ	0.6		–	Nm^{-1}
Thermal conductivity, K	5	0.0262	44.5	$Wm^{-1}K^{-1}$
Heat capacity, C_p	1425	1004	475	$Jkg^{-1}K^{-1}$
Diffusivity, α	$1.20 \cdot 10^{-6}$	$2 \cdot 10^{-5}$	$1.19 \cdot 10^{-5}$	$m^{-2}s^{-1}$
Latent heat of fusion, ΔH	770	–	–	$kJkg^{-1}$
Thermal inertia, ρC_p	4132500	–	3728750	$Jm^{-3}K^{-1}$
Initial diameter, d_i	20	–	–	μm
Initial temperature, T_i	2800	300	700	K
Impact velocity, V_i	40-250	–	–	ms^{-1}

One of the most important factors affecting the droplet spreading and solidification and thus the splat shape is the Reynolds number. In order to investigate the effect of this number on the droplet spreading and solidification, a number of simulations were performed by using different impact velocities ranging from 40 to 250 m/s. The investigated velocity range and the initial substrate temperature, are conditions for which no splashing was observed. The plasma-sprayed alumina splat has a circular disk shape allowing the axis-symmetric model approach to be applied.

Figure 3 shows the spread factor evolution for different Reynolds numbers. This factor characterizes the droplet spreading and therefore may serve to control the impact conditions. This figure shows that the spread factor increases rapidly in the first instants after impact, which

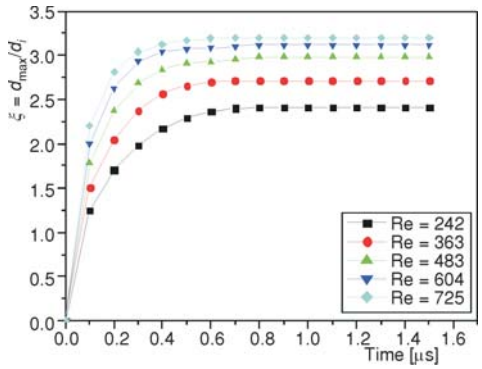

Figure 3. Spread factor evolution for different Reynolds numbers

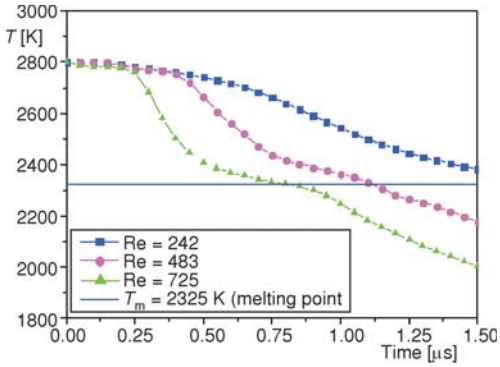

Figure 4. Droplet temperature evolution at 1 μm depth location from the substrate surface (z = 1 μm)

means that droplet starts spreading rapidly after impingement. This is due to the high compression that the droplet undergoes at the impact; a shock wave generates and proceeds upward inside the droplet. Thus, the elastic energy on the compressed liquid is then gradually transferred into the kinetic energy of lateral flow [24, 25].

Increasing the Reynolds number leads to a significant increase in the maximum spread factor and reduction of the required time for achieving the spreading.

The droplet temperature evolution at 1 μm depth location from the substrate surface (z = 1 μm) for different Reynolds number is shown in fig. 4. It can be seen from this figure that the solidification starts rapidly when increasing the Reynolds number. This is due to the enhancement of heat transfer from the droplet to the substrate and also to the spreading area which increases with the Reynolds number.

The simulations carried out for different values of Re permit to derive a new correlation that predicts the value of the maximum spread factor as function of Reynolds number for high impact velocities ranging from 40 m/s to 250 m/s such as that used in plasma spray process. A regression analysis carried out on all the numerical results computed for different Reynolds number show that the spread factor is in proportion of the 0.25 power of the Reynolds number leading to the expression: $\xi = 0.6166.\mathrm{Re}^{0.25}$.

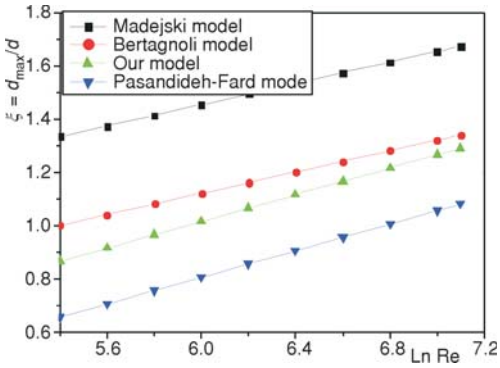

Figure 5. Spread factor *vs.* Reynolds number for different correlations

For comparison purpose, other relationships predicted or calculated in most cited research in the literature are plotted together with the correlation obtained in the present work in the same fig. 5.

The models of Madejski [13] and Bertagnoli [17] give higher values of the spread factor as compared to values given by our correlation. This may be due to several raisons. For example, in the analytical model of Madejski, the solidification was assumed to take place after the deformation, thus leading to a large value of ξ. In the numerical model of Bertagnoli, who used a finite elements method with a Lagrangian description to describe the motion of the viscous melt in a ce-

ramic droplet, the wetting effects were neglected. The model developed in the present wok takes into account both solidification and wetting effect, which have a major influence on the spreading and solidification process, and therefore may give better prediction.

The value of the exponent of Re derived in the correlation developed in the present work is similar to that of the analytical relationship derived by Pasandideh-Fard *et al.* [11], while the value of the coefficient differs slightly. This may be due to the inappropriate estimation of the thermal contact resistance; and the contact angle when it is not available in the literature. Thermal contact resistance was assigned zero in the model of Pasandideh-Fard, leading to a maximum heat transfer between the liquid and the substrate and to a decrease in the solidification time resulting in a decrease in the spreading length.

Conclusions

A 2-D axisymmetric model based on a finite element method was developed to simulate the droplet spreading and simultaneous solidification on a stainless steel substrate under plasma spraying conditions. The effect on the Reynolds number on the droplet spreading and solidification was investigated by using different impact velocities within the range 40 to 250 m/s. Thermal contact resistance, viscous dissipation, wettability and surface tension forces effects are taken into account in the model. A correlation that predict the spread factor as a function of the Reynolds number was obtained, $\xi = 0.6166\mathrm{Re}^{0.25}$. This correlation may give better prediction compared to others presented in the literature in the case of alumina droplets spreading on preheated substrate.

Acknowledgments

First author thanks the IUT Henri Poincaré Institute and the Longwy Energy Laboratory for support. PHC Program 30257 TE and AUF are also acknowledged.

Nomenclature

C – mushy zone constant,
C_p – specific heat, [Jkg^{-1}K^{-1}]
d_i – initial diameter, [m]
F – term source
FTS – surface tension forces, [N]
g – gravitational acceleration, [ms^{-2}]
H – latent heat of transition, [Jkg^{-1}]
l_0 – arbitrary thickness, [m]
L – latent heat, [Jkg^{-1}]
K – thermal conductivity, [Wm^{-2}K^{-1}]
k – average local slope of the curve at the interface
k_l – effective thermal conductivity, – [Wm^{-2}K^{-1}]
n – normal to the interface
p – pressure, [Pa]
Re – Reynolds number, ($=\rho u d_i/\mu$)
T – temperature, [K]
T_i – initial temperature, [K]
T_m – melting temperature, [K]
TCR – thermal contact resistance, [m^{2}KW^{-1}]
t – time, [s]
u – velocity fields, [ms^{-1}]
V_i – impact velocity, [ms^{-1}]
We – Weber number, ($=\rho u^2 d_i/\sigma$)

Greek symbols

β – volume fraction of the liquid phase
γ – stabilisation parameter, [ms^{-1}]
δ – Gaussian function
ε – interface thickness, [m]
θ – contact angle
μ – dynamic viscosity, [Pa·s]
ξ – spread factor
ρ – density, [kgm^{-3}]
σ – surface tension, [Nm^{-1}]
Φ – level set function
ϕ – arbitrary constant

Subscripts

i – initial condition
m – melting
s – substrate

References

[1] Fauchais, P., Understanding Plasma Spraying, *J. Phys. D: Appl. Phys, 37* (2004), 9, pp. 86-108
[2] Fataoui, K., *et al*., Simulation of the Thermal History and Induced Mechanical Stresses During a Plasma Spray Coating Process, *Phys. Chem. News, 40* (2008), March, pp. 23-28
[3] Fauchais, P., *et al*., Knowledge Concerning Splat Formation: An invited review, *J. Therm. Spray Technol. 13* (2004 b), 3, pp. 337-360
[4] Cedelle, J., *et al*., Investigation of Plasma Sprayed Coatings Formation by Visualization of Droplet Impact and Splashing on a Smooth Substrate, *IEEE Transactions on Plasma Science, 33* (2005), 21, pp. 414-415
[5] Mehdizadeh, N. Z., *et al*., Photographing Impact of Molten Molybdenum Particles in a Plasma Spray, *J. Therm. Spray Technol., 14* (2005), 3, pp. 354-361
[6] Sussman, M., *et al.*, A Level Set Approach for Computing Solutions to Incompressible Two-Phase Flow, *J. Comp. Phys, 114* (1994), pp. 146-159
[7] Zhao, Z., *et al*., Heat Transfer and Fluid Dynamics During the Collision of a Liquid Droplet on a Substrate: II Experiments, *Int. J. Heat Mass Transf., 39* (1996), 13, pp. 2791-2802
[8] Bussmann, M., *et al*., On a Three-Dimensional Volume Tracking Model of Droplet Impact, *Physics of Fluids, 11* (1999), 6, pp. 1406-1417
[9] Oukach, S., *et al*., Thermal Effects on the Spreading and Solidification of a Micrometric Molten Particle Impacting onto a Rigid Substrate, *FDMP: Fluid Dynamics & Materials Processing, 8* (2012), 2, pp. 173-195
[10] Jones, H., Cooling Freezing and Substrate Impact of Droplets Formed by Rotary Atomization, *J. Phys. D: Appl. Phys, 4* (1971), 11, pp. 1657-1660
[11] Pasandideh-Fard, M., *et al*., Capillary Effects During Droplet Impact on a Solid Surface, *Physics of Fluids, 8* (1996), 3, pp. 650-659
[12] Yoshida, T., *et al*., Integrated Fabrication Process for Solid Oxide Fuel Cells Using Novel Plasma Spraying, *Plasma Sources Science and Technology, 1* (1992), 3, pp 195-201
[13] Madejski, J., Solidification of Droplets on a Cold Surface, *Int. Journal of Heat and Mass Transfer, 19* (1976), 9, pp. 1009-1013
[14] Zhang, H., Theoretical Analysis of Spreading and Solidification of Molten Droplet during Thermal Spray Deposition, *Int J Heat Mass transfer, 42* (1999), 14, pp. 2499-2508
[15] Liu, H., *et al.*, Numerical Simulation of Impingement of Molten Ti, Ni and W Droplets on a Flat Substrate, *J. Therm, Spray Technol., 2* (1993), 4, pp 369-377
[16] Trapaga, G., Szekely, J., Mathematical Modeling of the Isothermal Impingement of Liquid Droplets in Spraying Processes, *Metall. Trans., 22B* (1991), 6, pp. 901-914
[17] Bertagnolli, M., *et al*., Modeling of Particles Impacting on a Rigid Substrate under Plasma Spraying Conditions, *J. Thermal. Spray Technol, 4* (1995), 1, pp. 41-49
[18] Watanabe, T., *et al.*, Deformation and Solidification of a Droplet on a Cold Substrate, *Chem. Eng. Sci., 47* (1992), 12, pp. 3059-3065
[19] Sethian, J., *Level Set Methods*, Cambridge University Press, Cambridge, UK, 1996
[20] Voller, V. R., *et al*., An Enthalpy Method for Convection-Diffusion Phase Change, *Int. J. Numerical Methods in Engineering, 24* (1987), 1, pp. 271-284
[21] Oukach, S., *et al.*, Thermomechanical Modelling of the Formation of a Lamella in the Plasma Sprayhing Conditions, *Phys. Chem. News, 67* (2013), 1-2, pp. 113-119
[22] Oukach, S., *et al*., Numerical Simulation of Drop Splashing on a Wall, *Proceedings*, 1er Congrès de l'Association Marocaine de Thermique (AMT 2010), Settat, Morocco, 2010, pp. 101-108
[23] Mebdoua, Y., Numerical Study of the Thermal Phenomena Controlling the Solidification of a Lamella during Thermal Protrusion: Application to the Formation of the Deposit, Ph. D. thesis, University of Limoges. France, 2008
[24] Engel, O. G., Initial Pressure, Initial Flow Velocity, and the Time Dependence of Crater Depth in Fluid Impacts, *J. Appl. Phys. 38* (1967), 19, pp. 3935-3940
[25] Heymann, F. J., High-Speed Impact Between a Liquid Drop and a Solid Surface, *J. App.Phys, 40* (1969), 13, pp. 5113-5122

Paper submitted: May 21, 2014
Paper revised: July 5, 2014
Paper accepted: August 17, 2014